BULLETIN OF THE POLISH ACADEMY OF SCIENCES
TECHNICAL SCIENCES, Vol. 67, No. 2, 2019
DOI: 10.24425/bpas.2019.128607

Static load test curve analysis based on soil field investigations

P. SIEMASZKO* and Z. MEYER

West Pomeranian Institute of Technology Szczecin, Faculty of Civil Engineering and Architecture, Piastów 50, 70-311 Szczecin

Abstract. This paper expands the M-K curve theory with examples of the most commonly mentioned pile-soil mechanics behaviours in the literature and their corresponding κ_2 variations. A brief introduction shows the history of the Meyer-Kowalow theory and its basic assumptions. This is followed by the relationship between in situ investigation CPT results, with parameters C_1, C_2, C_t used to approximate the load-settlement curve according to the M-K theory. The Meyer-Kowalow curve satisfies asymptotic behaviour for small loads, where linear theory applies, and for limit loads, when pile displacement is out of control. Essential in the description are constant parameters C, which refer to the aggregated Winklers modulus, *Ngr* limit loads and *k*, which is crucial for static load test results. For this reason, the authors sought to calculate the κ value based upon soil mechanics principles. This article shows methods for checking statistical mathematical calculations, published earlier by Meyer using CPT investigations. It presents real case calculations and directions for future planned research.

Key words: static pile test, skin friction, static load test curve, soil characteristics.

1. Preface

The mechanism of pile base and shaft stress formation is a crucial problem in estimating the pile-bearing capacity process. There are many authors, whose research has focused on this topic [1–5, 9–11, 13]. Most of these works revolve around the static load pile test, with fewer discussing an analytical approach to shaft and base resistance regarding soil mechanics behaviour. The pile static test is recommended as the primary method of verifying pile-bearing capacity. Most pile static test results indicate that dimensions could be changed, but no indication is given on how to prove it. There is lack of equational relationship between pile behaviour and soil characteristics that would allow for the conversion of pile dimensions with the use of the *Q*–*s* diagram for a given soil configuration.

Previous works have formulated theories with which to predict pile-bearing capacity using the results of CPT investigation [15, 16, 18, 19]. The authors [15] gathered the theories and subjected them to comparison. The author [17] compared the Eurocode 7 and Polish Code standard methods. All of these works prove that there is need for a comprehensive theory, which would allow for predicting pile-bearing capacity with greater accuracy. In these works, the description of the analytical curve describing the relationship between load and settlement is lacking.

Jean-Louis Briaud [25] presented a graph, which allows the formulation of the following theory. While the entire bearing capacity is composed of aggregated toe and skin, it can be assumed that skin friction, in earlier phases of pile settlement, reaches its extreme value and accounts for the principal part of pile-bearing capacity. With increasing movement of the pile, toe capacity increases to the point where it may be more significant than skin friction resistance, although settlement is going to exceed the values permitted by the Codes in this case. Considerable effort should be devoted to finding tools that would estimate the extreme value of skin friction capacity. The extreme value of skin friction is the point at which the total pile capacity has the greatest usable value in terms of engineering and economical exploitation.

Bearing this in mind, Meyer and Kowalow's objective was to find the curve that would allow one to describe the situation shown in the graph by Jean-Louis Briaud [25]. The authors of this paper focused on formulating a theory regarding the M-K curve (Meyer-Kowalow) that might be used to approximate the pile static load test curve. M-K curve parameters can be established using soil characteristics from field investigations. This may be the way to arrive at a more physical approach to the M-K curve, using equations of soil mechanics as a base.

2. M-K curve

In the literature there are plenty of results from experimental pile investigations. They provide examples of the relationship between the axial force at the head and pile settlement. The works by Chin [22] and Davisson [23] present methods of estimating the failure load of piles based on the static load test. They have their own limitations and do not fully describe the problem of the appropriate estimation of pile-bearing capacity. The curve presented by Chin [22] is a Meyer-Kowalow curve variation, where $\kappa = 1$; therefore, it cannot be used as a general example to cover this case. The base and shaft stress forming mechanisms, including increasing settlement, in the entire range of the load applied to the head of the pile lack theoretical underpinnings.

*e-mail: pw.siemaszko@gmail.com

Manuscript submitted 2018-11-09, revised 2019-02-13, initially accepted for publication 2019-03-18, published in April 2019.

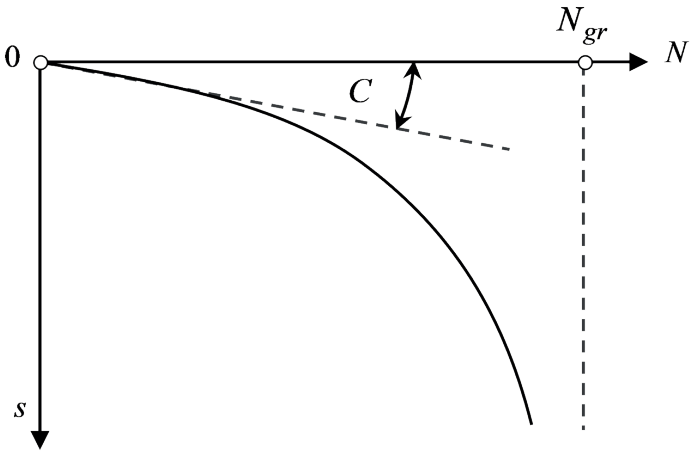

Fig. 1. Scheme of the M-K static load test curve

The course of the function of static load test curve extrapolated using M-K theory is shown on Fig. 1.

Parameter C, used in the M-K curve, may be identified with Winkler modulus, as it aggregates toe and skin resistance during pile settlement. Later on in this paper, parameter C will be referred to as the reversed aggregated Winkler modulus. Parameter C consists of two factors: C_1 which stems from toe settlement, and C_t which stems from skin settlement. The exact derivation is shown in (30), which demonstrates a strict relationship between those factors.

The M-K curve equation is formulated as [6, 8–11, 13]:

$$s = C \cdot N_{gr} \cdot \frac{\left(1 - \frac{N}{N_{gr}}\right)^{-\kappa} - 1}{\kappa} \tag{1}$$

where: s – settlement of head of the pile [mm];
C – parameter that is reversed aggregated Winklers modulus $\left[\frac{m}{MN}\right]$, which is specified later in the paper;
N_{gr} – axial force, M-K curve vertical asymptote [MN];
κ – parameter showing the proportion of base and shaft resistance.

The M-K curve possesses a vertical asymptote, that is:

$$N = N_{gr} \quad \text{and crosswise} \tag{2}$$

$$s = C \cdot N. \tag{3}$$

It can be proven that:

$$\lim_{N \to 0} s(N) = C \cdot N \quad \text{and} \tag{4}$$

$$\lim_{N \to N_{gr}} s(N) = \infty. \tag{5}$$

This means that the M-K curve depicts the physical aspects of the analysed mechanism of pile settlement under axial load applied at the top of the pile. For $N \to 0$, small displacement and linear relationship of load settlement are observed. For $N \to N_{gr}$, settlement increases out of control and the pile loses its bearing capacity.

The principal task of the M-K curve approximation is to estimate N_{gr} value and predict the mobilisation of pile base and shaft capacity. The first step is to estimate the M-K curve parameters using static load test results. The output results are $\{Q_i; s_i\}$ resultant values. Mathematical analysis can be applied to arrive at the solution of this task.

This problem has been the focus of many works [6, 7]. Their outcome states that with the set of values $\{Q_i; s_i\}$ the M-K curve parameters: C, N_{gr}, κ can be established.

The main problem addressed in this article is to analyse whether the M-K curve parameters can be found based on in-situ investigation results with the application of a theory of soil mechanics. For small loads, when the correlation between load and settlement is linear, the C parameter represents the reversed aggregated Winkler modulus [12]. Due to this fact, we can calculate its value using a solution proposed by Bousinessq [6, 13].

In Fig. 2, the distribution of shaft and base pile stress is presented.

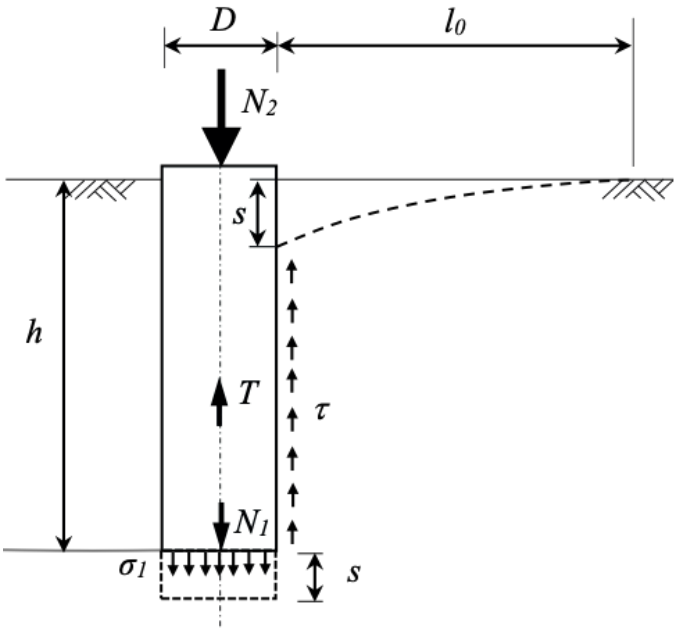

Fig. 2. Distribution of load and stress within pile-soil interaction

The basic assumption of this article, proposed in this diagram, is that shaft stress is the result of soil displacement around the pile. In the literature, there are many approaches to the representation of the foundation-soil interaction mechanism and stress distribution. Most numerical methods make use of the Winkler modulus, which is widely debated in the paper [21]. Some use statistical methods [20, 24]. A diagram proposing the application of the Winkler modulus is presented in the work [14].

The article by Meyer and Siemaszko analyses a case in which a reaction in the base of a pile is caused by pile and soil

interaction. The authors propose that soil displacement and, therefore, shaft stress is caused by settlement s at the surface, which occurs after loading the head of the pile with load N_2. This displacement is captured by equation [6, 13]:

$$s = \frac{\tau}{G} \cdot l \tag{6}$$

$$G = \frac{E_t}{2(1+v)} \tag{7}$$

where: l – horizontal soil displacement range [m];
G – shear modulus, according to Kirchoff [MPa];
υ – Poisson constant;
τ – skin stress on the surface of the pile shaft [MPa].

In previous work by Meyer [6], it has been proven that the range of soil displacement l, based on linear elasticity, can be presented as:

$$l = D \cdot \frac{1 + 3\ln\left(\frac{4h}{D}\right)}{2(1+v)} \tag{8}$$

where: h – pile length [m];
D – pile diameter [m].

It can be proven that in terms of practical engineering calculations, the equation can be simplified:

$$l \cdot 2 \cdot (1+v) = 3{,}68 \cdot \left(\frac{h}{D}\right)^{0{,}215} \cdot D. \tag{9}$$

If:

$$10 < \left(\frac{h}{D}\right) < 40. \tag{10}$$

Equation (6) can be presented now as:

$$\tau = \frac{1}{1.738 \cdot \left(\frac{h}{D}\right)^{1/3}} \cdot \frac{E_t \cdot s}{D}. \tag{11}$$

For further analysis it is convenient to note it as:

$$T = \int_0^h \tau \cdot \pi D \cdot dz. \tag{12}$$

For practical engineering calculations, upon analysing laboratory and field results [2, 3, 11, 12], the following can be assumed:

$$E_\tau = 4 \cdot \beta \cdot q_c(z) \tag{13}$$

where: $q_c(z)$ – cone resistance at "z" depth [MPa];
$\beta = 1 \div 2$ – parameter depending on pile boring technology used.

Moreover, it is assumed that the average cone resistance of the pile length is:

$$\int_0^h q_c(z) \cdot dz = \overline{q_c} \cdot h. \tag{14}$$

After sorting all the equations (11–14), the following can be obtained:

$$T = \frac{4\pi \cdot \beta}{3{,}68} \cdot \left(\frac{h}{D}\right)^{0{,}785} \cdot D \cdot s \cdot \overline{q_c}. \tag{15}$$

The above equation (15) can be used to estimate the shaft resistance of the pile, with the known distribution of vertical cone resistance $q_c(z)$. In (15), the following symbols are used: relationship between length and diameter of a pile h/D, diameter of pile D, settlement of pile s, average vertical CPT measurement $\overline{q_c}$. The equation structure shows that pile shaft resistance is directly proportional to all values mentioned beforehand.

Pile base resistance is the second value that describes the bearing capacity of a pile. Pile base resistance is the reaction of soil to load N_1.

Experimental analysis [26] shows that the loading pile causes areas of plastic soil to form under the pile base, as shown in Fig. 3, whose diameter is $D_p > D$. The assumption is made:

$$s = \frac{4}{\pi} \cdot \frac{N_1}{E_p \cdot D_p} \tag{16}$$

where: E_p – soil elastic modulus under pile base [MPa];
N_1 – load value at the pile base [MN];
D_p – plastic soil area diameter [m].

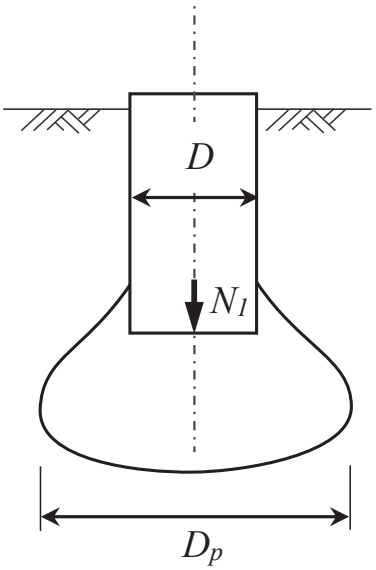

Fig. 3. Scheme of base settlement of a pile [8]

The soil elastic modulus was estimated based on EC7 and experimental results [27, 28]. The following is obtained:

$$E_p = 4 \cdot q_b \cdot \left(1 + \frac{1}{4} q_b^{1/3}\right) \tag{17}$$

q_b – cone resistance representing soil under pile base.

The value of D_p was estimated using numerical methods and experimental results [26]. For practical engineering calculations, the following relationship was examined:

$$D_p = D \cdot \left(1 + \frac{2q_b}{1 + q_b}\right) \tag{18}$$

or its more general form:

$$D_p = D \cdot f(\kappa_2). \tag{19}$$

In which [27]

$$f(\kappa) = 1 + \ln(1 + \kappa_2). \tag{20}$$

Based on (16) and (17), the following is obtained:

$$N_1 = \frac{\pi}{4} \cdot s \cdot D_p \cdot 4 \cdot q_b \cdot \left(1 + \frac{1}{4} q_b^{1/3}\right). \tag{21}$$

Under these assumptions, the relationship between shaft resistance and toe resistance can be shown as:

$$\frac{T}{N_1} = \frac{4\beta}{3{,}68} \cdot \left(\frac{h}{D}\right)^{0{,}785} \cdot \frac{\overline{q_c}}{q_b} \cdot \frac{D}{D_p} \cdot \frac{1}{1 + \frac{1}{4} q_b^{\frac{1}{3}}}. \tag{22}$$

Equation (22) is a basic relationship, which shows the proportional share of shaft and toe pile resistance for minor loads with respect to the linear elasticity theory. That equation shows also the values of the reversed aggregated Winkler modulus for the shaft and toe of the pile.

3. Relationship between M-K curve parameters

Based on laboratory research [8], it can be assumed that the M-K curve allows for the definition of not only the Q–s curve of static load, but also the mobilisation of pile and shaft resistance. According to Fig. 2, an assumption can be made:

$$N_2(s) = N_{gr2} \cdot \left[1 - \left(1 + \frac{\kappa_2 \cdot s}{N_{gr2} \cdot C_2}\right)^{-\frac{1}{\kappa_2}}\right] \tag{23}$$

$$N_1(s) = N_{gr1} \cdot \left[1 - \left(1 + \frac{\kappa_1 \cdot s}{N_{gr1} \cdot C_1}\right)^{-\frac{1}{\kappa_1}}\right]. \tag{24}$$

In equations (23–29) there are additional parameters:

- C_1 – reversed aggregated Winklers modulus for N_1 force at the pile base $\left[\frac{m}{MN}\right]$;
- C_2 – reversed aggregated Winklers modulus for N_2 force at the head of the pile $\left[\frac{m}{MN}\right]$;
- N_1, N_2 are loads respectively at the base and head of the pile [MN].

Furthermore, there is κ_1 for $s = f(N_1)$ and κ_2 for $s = f(N_2)$. T is the symbol for mobilising shaft resistance [MN]. According to C_1 and C_2 parameters, the C_t parameter is added, which corresponds to T force $\left[\frac{m}{MN}\right]$.

In classical mechanics, the Winklers modulus is related to pile settlement caused by load at the head of the pile. The aggregated Winklers modulus presented in this article includes shaft resistance of a pile. Relationship T/N_1 (22) is considered to be a contributing factor of aggregated Winklers modulus.

Pile-bearing capacity [28] analysis proves that shaft resistance is more significant than toe resistance, while toe resistance value is around 20% that of pile head load. Further analysis of this pile-bearing capacity mechanism leads to the implementation of the C_1, C_2, C_t coefficients later on in this article.

In consequence, the shaft resistance equation assumes the following form:

$$T(s) = N_2(s) - N_1(s). \tag{25}$$

Figure 4 shows curves estimated with (23–25).

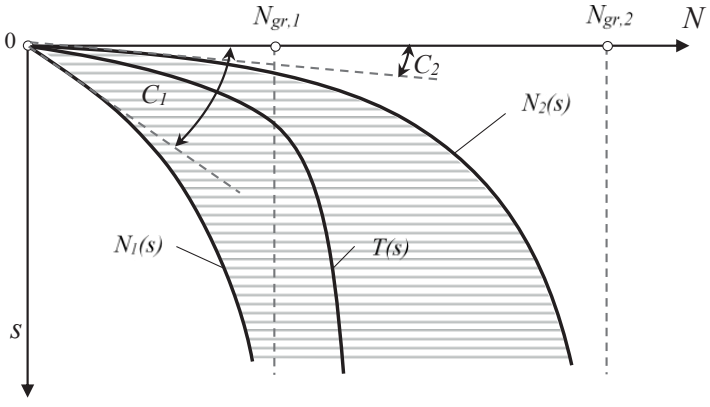

Fig. 4. Graph of functions describing pile base and shaft resistance for static load test results Q–s

According to the linear elastic theory, the displacement for small loads range is:

$$\lim_{s \to 0} N_2(s) = \frac{s}{C_2} \tag{26}$$

$$\lim_{s \to 0} N_1(s) = \frac{s}{C_1} \tag{27}$$

and:

$$\lim_{s\to 0} T(s) = \frac{s}{C_2} - \frac{s}{C_1}. \tag{28}$$

For further analysis, it is convenient to formulate:

$$\lim_{s\to 0} T(s) = \frac{s}{C_2} - \frac{s}{C_1} = \frac{s}{C_t} \tag{29}$$

then

$$\frac{1}{C_2} = \frac{1}{C_1} + \frac{1}{C_t}. \tag{30}$$

These steps added the following parameters to the pile and soil mechanics description: C_1, C_2, C_t.
All of these parameters constitute the reversed aggregated Winkler modulus and are correlated with soil reaction to the forces N_1, N_2, T respectively.

With respect to the analysis of (25÷29), there are additional relationships that can be used [8]:

$$\frac{C_1}{C_2} = (1+\kappa_2)^2, \tag{31}$$

$$\kappa_1 = \ln(1+\kappa_2), \tag{32}$$

and under average conditions

$$N_{gr1} = N_{gr2} \cdot \frac{1+\kappa_1}{(1+\kappa_2)^2}. \tag{33}$$

Additionally, (30) yields:

$$\frac{C_1}{C_2} = 1 + \frac{C_1}{C_t}. \tag{34}$$

From (21), stems the following:

$$\frac{N_1}{s} = C_1^{-1} = \pi D_p q_b \cdot \left(1 + \frac{1}{4} q_b^{1/3}\right). \tag{35}$$

From (15), stems the following:

$$\frac{T}{s} = C_t^{-1} = \frac{4\pi\cdot\beta}{3{,}68} \cdot \left(\frac{h}{D}\right)^{0{,}785} \cdot D \cdot \overline{q_c}. \tag{36}$$

Therefore, (34) can be presented as:

$$\frac{C_1}{C_2} = 1 + \frac{T}{N_1}. \tag{37}$$

and, finally, the following relationship is obtained:

$$\frac{C_1}{C_2} = 1 + \frac{4\beta}{3{,}68} \cdot \left(\frac{h}{D}\right)^{0{,}785} \cdot \frac{\overline{q_c}}{q_b} \cdot \frac{D}{D_p} \cdot \frac{1}{1+\frac{1}{4}\cdot q_b^{\frac{1}{3}}}. \tag{38}$$

Substituting (31) for the above relationships, κ_2 can be estimated as follows:

$$(1+\kappa_2)^2 - 1 = 1 + \frac{4\beta}{3{,}68} \cdot \left(\frac{h}{D}\right)^{0{,}785} \cdot \frac{\overline{q_c}}{q_b} \cdot \frac{D}{D_p} \cdot \frac{1}{1+\frac{1}{4}\cdot q_b^{\frac{1}{3}}}. \tag{39}$$

Upon combining the formulas listed above, the C_1/C_2 relationship is obtained, which varies according to the pile soil mechanism conditions. It allows for the estimation of the value of κ_2, that is responsible for showing the settlement increase rate in the M-K theory. The following is obtained:

$$(1+\kappa_2)^2 - 1 = \frac{T}{N_1}. \tag{40}$$

Equations (39) and (40) together form the basic description of the shaft and base resistance relationship. This is based on static load tests for small displacements.

4. Practical application of κ_2 equation

The previous section showed the method of estimating the κ_2 parameter with in-situ test results. Equation (39) contains D_p, which represents the diameter of the plastic soil area formed under the base of the pile. The first step was an attempt to apply the presented method in order to describe the most common schemes found in the literature of soil formation around the pile base. The practical applications of D_p schemes are shown on Fig. 5.

The examples shown in Fig. 5 differ from the mechanism of soil behaviour around the pile base when it reaches its plastic state. κ_2 relationships, shown further in this section, present differences in values for different soil pile interactions. The structure of equations (42–45) show that κ_2 value is dependent on H/D and $\overline{q_c}/q_b$ ratios. The most probable case is the third [26] one. It indicates that there is movement of soil from the pile base to the lower shaft section.

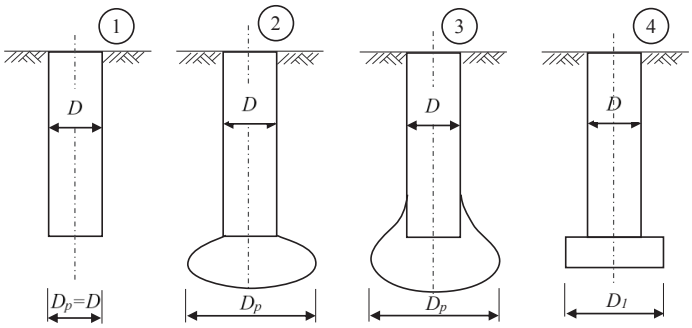

Fig. 5. Various examples of soil behaviour under the base of a pile

The equations describing situations 1) to 4) are as follows:

$$\left.\begin{aligned} &:1) \quad D_p = D \\ &:2) \quad D_p = D\left(1+\frac{2q_b}{1+q_b}\right) \\ &:3) \quad D_p = D\left(1+\kappa_1\right) \\ &:4) \quad D_p = D_1 \end{aligned}\right\}. \tag{41}$$

Based on each equation, the following κ_2 equations are derived:
Case 1):

$$\kappa_2 = \left[\frac{4\beta}{3{,}68}\cdot\left(\frac{h}{D}\right)^{0{,}785}\cdot\frac{\overline{q_c}}{q_b}\cdot\frac{1}{1+\frac{1}{4}q_b^{\frac{1}{3}}}\right]^{1/2} - 1 \tag{42}$$

Case 2):

$$\kappa_2 = \left[\frac{4\beta}{3{,}68}\cdot\left(\frac{h}{D}\right)^{0{,}785}\cdot\frac{\overline{q_c}}{q_b}\cdot\cdot\cdot\frac{1}{\left(1+\frac{2q_b}{1+q_b}\right)\left(1+\frac{1}{4}q_b^{\frac{1}{3}}\right)}\right]^{1/2} - 1 \tag{43}$$

Case 3):

$$\kappa_2 = \left[\frac{4\beta}{20{,}86}\cdot\left(\frac{h}{D}\right)^{0{,}785}\cdot\frac{\overline{q_c}}{q_b}\cdot\frac{1}{1+\frac{1}{4}q_b^{\frac{1}{3}}}\right]^{3/5} - 1 \tag{44}$$

Case 4):

$$\kappa_2 = \left[\frac{4\beta}{3{,}68}\cdot\left(\frac{h}{D}\right)^{0{,}785}\cdot\frac{\overline{q_c}}{q_b}\cdot\frac{D}{D_1}\cdot\frac{1}{1+\frac{1}{4}q_b^{\frac{1}{3}}}\right]^{1/2} - 1 \tag{45}$$

The relationships shown above can be used not only to estimate the κ_2 value for given soil characteristics, but also when the soil conditions or pile dimensions are changed.
Based on (39÷45), for practical engineering calculations, the M-K curve parameters can be estimated, derived from static load test curve approximations.

The κ_2 relationships can be used if we know the M-K curve parameters. They may be suitable for presenting the following relationships:
– $N_1(s)$ pile base resistance according to settlement;
– $N_2(s)$ load at the head of the pile according to settlement;
– $T(s)$ pile shaft resistance according to settlement.
Only C, κ, N_{gr} parameters are needed for a proper estimation. C_2, κ_2, N_{gr2} are obtained using mathematical statistics methods for the load-settlement curve [28], and also C_1, κ_1, N_{gr1} which appears to be the main problem. According to [27], the following relationships can be used:

$$\frac{N_{gr2}}{N_{gr1}} = \frac{1+\kappa_1}{\left(1+\kappa_2\right)^2} \tag{46}$$

$$C_1 = \frac{1}{\pi D q_b\cdot\left(1+\kappa_2\right)^{\frac{3}{4}}\cdot\left(1+\frac{1}{4}q_b^{\frac{1}{3}}\right)} \tag{47}$$

$$C_2 = C_1/\left(1+\kappa_2\right)^2. \tag{48}$$

As a verification for pile base bearing capacity N_{gr1}, the following equation can be used:

$$N_{gr1} = \frac{1}{2\pi}\cdot q_b\cdot D^2\cdot\left(\frac{h}{D}\right)^{1/3}. \tag{49}$$

5. Sample calculations

For a typical task, the results of a static load test are provided, giving the set $\{Q_i; s_i\}$. With the use of statistical methods, the following are calculated: C_2, N_{gr2}, κ_2 based on the set $\{Q_i; s_i\}$. The curve Q–s can be estimated. In order to estimate another $N_1\ (s)$ and $T\ (s)$ curve, the M-K curve parameters for the pile toe are needed.

$$\kappa_1 = \ln\left(1+\kappa_2\right), \tag{32}$$

$$N_{gr1} = N_{gr2}\cdot\frac{1+\kappa_1}{\left(1+\kappa_2\right)^2}. \tag{33}$$

For the calculation of N_{gr1} the following equation is used [27]:

$$N_{gr1} = \frac{C_2}{C_1}\cdot N_{gr2}\cdot\left[1+0{,}1435\cdot\left(\frac{H}{D}\right)^{1/3}\cdot\kappa_2^{0{,}5}\right]. \tag{50}$$

With these values, $N_2\ (s)$, $N_1\ (s)$, $T\ (s)$ curves can be plotted. Examples of curves with M-K constants values are presented in Fig. 6.

Table 1 presents real case values of static pile load tests. Table 2 shows the M-K approximation parameters for a real case pile that the authors used for their analysis.
The next step is verification with (49):

$$N_{gr1} = \frac{1}{2\pi}\cdot 16\cdot 0{,}51^2\cdot\left(\frac{11{,}5}{0{,}51}\right)^{\frac{1}{3}} = 1871{,}21\ \text{kN}.$$

There is a minor difference of 3% between values obtained with statistical calculations and (49) verification. It can be assumed that the values are correct.

Table 3 presents the values obtained during static pile load tests and the calculations of values $N_1(s)$, $N_2(s)$, $T(s)$ obtained with (23–25) for every settlement value.

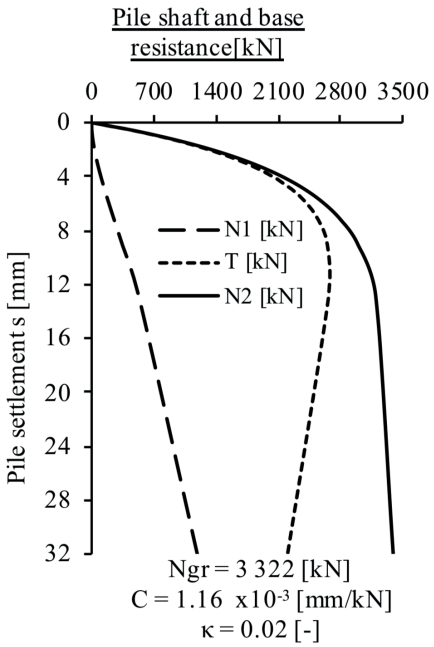

Fig. 6. M-K approximation curves of pile resistance components with M-K constant values

Table 1
Static pile load test results

Pile static load test results $\{N_i; s_i\}$ values			
N_i [kN]	s_i [mm]	N_i [kN]	s_i [mm]
120	0,3	700	1,9
220	0,5	800	2,35
320	0,8	940	3
420	1	1060	3,7
500	1,25	1200	4,31
600	1,6		

Table 2
M-K approximation parameters

Pile properties	M-K approximation results
H = 11,5 m	C_2 = 0,002376686
D = 0,51 m	Ngr_2 = 1900
CPT results	$\varkappa_2$ = 0,080366011
q_b = 16 kN/m^2	C_1 = 0,002774046
	Ngr_1 = 1814,926718
	$\varkappa_1$ = 0,077299883

Figure 7 plots all graphs with N_{gr1}, N_{gr2} results. The N_{gr2} value was obtained with statistical methods [27, 28] and N_{gr1} using equation (50), as presented earlier. Values were extrapolated using M-K approximation to show extreme values of $T(s)$.

Table 3
Calculation results of static load test values extrapolated with M-K approximation and bearing capacity components

Pile static load test results $\{N_i; s_i\}$ values and bearing capacity components N_1, N_2, T values			
s_i [mm]	$N_2(s)$ [kN]	$N_1(s)$ [kN]	T(s) [kN]
0,30	121,8104	104,75239	17,058
0,50	198,3151	170,95785	27,3572
0,80	306,4828	265,14289	41,3399
1,00	374,4547	324,69375	49,7609
1,25	455,0479	395,68882	59,3591
1,60	560,2465	489,0279	71,2186
1,90	643,8427	563,77687	80,0658
2,35	758,8507	667,51723	91,3334
3,00	905,352	801,3405	104,011
3,70	1040,72	926,88845	113,832
4,31	1142,52	1022,6797	119,84
4,81	1216,256	1092,9016	123,355
5,30	1281,047	1155,2537	125,794
6,01	1363,442	1235,53	127,912
6,41	1404,578	1276,0676	128,51
6,91	1451,271	1322,495	128,776
7,43	1494,835	1366,2448	128,59
7,96	1534,574	1406,5594	128,015
8,40	1564,37	1437,0664	127,304
8,50	1570,77	1443,6517	127,118
9,23	1613,675	1488,1364	125,539
9,80	1642,973	1518,8748	124,098
10,00	1652,472	1528,9096	123,562
10,50	1674,599	1552,4285	122,17
11,01	1694,984	1574,2865	120,698
11,42	1709,929	1590,4369	119,492
12,01	1729,406	1611,6623	117,744
12,53	1744,792	1628,5823	116,209
12,90	1754,823	1639,6949	115,128
13,40	1767,282	1653,592	113,69
14,50	1790,811	1680,1615	110,65
15,10	1801,712	1692,6329	109,079
16,00	1815,917	1709,0667	106,851

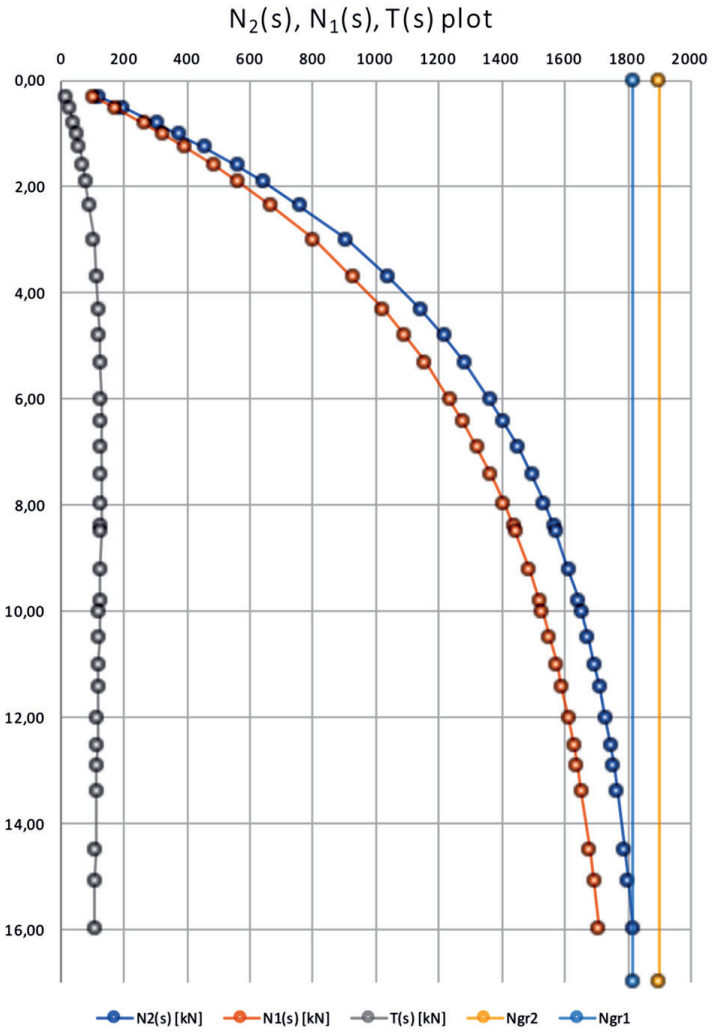

Fig. 7. $N_1(s)$, $N_2(s)$, T(s) graphs with N_{gr1}, N_{gr2} values

6. Conclusions

1) This work presents an analysis of the Meyer-Kowalow curve, used to approximate static load tests of pile data.
2) An assumption was made that for every $\{Q_i; s_i\}$ set obtained with a static pile load test, there is a set of values C_2, N_{gr2}, κ_2 obtained via statistical mathematical methods [27].
3) A detailed analysis of the principles of pile toe and pile shaft resistance formation for small load values within the linear soil mechanics rules took place. The results of this analysis indicate that in comparison to the classical approach of soil response modelling, there is a need for the implementation of aggregated Winkler modulus, which is a contributing factor not only to toe pile resistance, but shaft resistance as a result of soil deflection.
4) In this work, four examples of pile and soil interaction were presented in Fig. 5, with the third being laboratory tested [26] and deemed as the most probable to occur. This means that there is soil movement from under the pile base to lower parts of its shaft. The κ_2 relationships (42–45) presented can be used to verify the C_2, N_{gr2}, κ_2 values obtained with statistics from the $\{Q_i; s_i\}$ set from the pile static test load. They may be useful for examining the accuracy of static pile load tests in addition to CPT verification, if results are available.
5) In practice, the application of the presented method allows the estimation of shaft and base resistance with settlement, when settlement is caused by load at the head of the pile. The presented example [25] suggests that $T(s)$ can reach extremum and assumes that it can exceed the maximum shaft resistance value caused by friction.
6) Further analysis will be focused on implementing the presented method to estimate the resistance of piles made with various technologies and in various soil environments. There are expectations to learn more about N_{gr2} estimation, and limit pile bearing-capacity calculation. A lot of attention will be paid in estimating the maximum allowable load that can be put at the head of the pile, in order not to exceed the second limit state settlement value.
7) There is a plan to test piles in the field to obtain a set of $\{Q_i; s_i\}$ values and determine if there is need for verification with independent soil from in situ investigations.

References

[1] W. Bogusz and S. Łukasik, "Approximation of pile bearing capacity based on field soil investigations based on PN-EN-1997 and PN-B-02482", *Environmental Engineering*, pp. 177–183, Białystok (2013), [in Polish].
[2] K. Gwizdała, "Pile foundations", *Wydawnictwo Naukowe PWN*, Warszawa, (2010), [in Polish].
[3] K. Gwizdała, "Polish experience in the assessment of pile bearing capacity and settlement of the pile foundation", 2016.
[4] K. Gwizdała and A. Krasiński, "Bearing capacity of displacement piles in layered soils with highly diverse strength parameters", *Pierre Delage*, *Jacques Desrues*, *Roger Frank*, *Alain Puech F.S. (Ed.)*, *Proceedings of the 18th International Conference on Soil Mechanics and Geotechnical Engineering Conference on Soil Mechanics and Geotechnical Engineering*, *Presses des Ponts*, Paris, (2013).
[5] A. Krasiński, "Proposal for Calculating the Bearing Capacity of Screw Displacement Piles in Non-Cohesive Soils Based on Cpt Results", *Stud. Geotech. Mech. XXXIV* (2012).
[6] Z. Meyer, "Shaft and base of a pile stress analysis of a single pile based on Boussinesq linear theory", *XVIII Scientific Seminar Regional Problems Of Environmental Engineering*, Szczecin (2015), [in Polish].
[7] Z. Meyer and K. Stachecki, "Static load test curve (Q–s) conversion in to pile of different size", *Ann. Warsaw Univ. Life Sci. – SGGW. 50*, pp. 171–182. (2018).
[8] Z. Meyer and K. Żarkiewicz, "Skin and Toe Resistance Mobilisation of Pile During Laboratory Static Load Test", *Stud. Geotech. Mech. 40*, pp. 1–5, 2018.
[9] P. Rychlewski, "Investigation of test piles", *Nowoczesne Budownictwo Inżynieryjne*, pp. 72–74, Kraków, 2009, [in Polish].
[10] G. Szmechel, "Estimation of maximal pile bearing capacity based on static pile load test in restricted settlement range", *West Pomeranian Institute Of Technology Szczecin*, 2014, [in Polish].
[11] Z. Wiłun, "Geotechnics outline", *Wydawnictwa Komunikacji Łączności*, 2008, [in Polish].

[12] K. Żarkiewicz, "Laboratory research of toe resistance based on static pile load tests in different schemes", *Second International Conference: Challenges in Geotechnical Engineering*, pp. 80–81 (2017).
[13] K. Żarkiewicz, "Estimation of pile base and shaft bearing capacity using pile settlement curve", *Inżynieria Morska i Geotechnika 3*, pp. 224–229 (2018).
[14] S. Chandra, "Modeling of soil behavior", *Presentation on* Indian Institute of Technology (2014).
[15] A. Eslami, B.H. Fellenius, "Pile capacity estimated from CPT data – Six methods compared", *International Society for Soil Mechanics and Geotechnical Engineering*, pp: 91–94 (1997).
[16] A. Eslami, E. Aflaki, and B. Hosseini: "Evaluating CPT and CPTu based pile bearing capacity estimation methods using Urmiyeh Lake Causeway records", *Scientia Iranica Volume 18*, *Issue 5*, pp:1009–1019, October 2011.
[17] B. Czado and B. Wrana, "Bearing capacity of pile foundations based on CPT results in accordance to Polish standards and Eurocode 7", *AGH Journal of Mining and Geoengineering*, vol. 36 No. 2, pp. 111–119, Kraków (2012).
[18] I.N. Obeta, M.E. Onyia, D.A. Obiekwa, "Comparative analysis of methods of pile-bearing capacity evaluation using CPT logs from tropical soils", *Journal of the South African Institution of Civil Engineering vol. 60* (2018).
[19] A.S. Azizkandi, A. Kashkooli, and M.H. Baziar, "Prediction of Uplift Pile Displacement Based on Cone Penetration Tests (CPT)", *Geotechnical and Geological Engineering*, vol. 32, Issue 4, pp. 1043–1052 (2014).
[20] A. Misra, A.L. Roberts, "Axial service limit state analysis of drilled shafts using probabilistic approach", *Geotechnical and Geological Engineering*, vol. 24, pp. 1561–1580 (2006).
[21] S.J. Matysiak, R. Kulchytsky-Zhygailo, and D.M. Perkowski, "Stress distribution in an elastic layer resting on a Winkler foundation with an emptiness", *Bull. Pol. Ac.: Tech.*, vol. 66, No. 5, p. 721–727 (2018).
[22] F.V. Chin, "Estimation of the Ultimate Load of Piles Not Carried to Failure", *Proceedings of 2nd Southeast Asian conference on Soil Engineering*, pp. 81–90 (1970).
[23] M.T. Davisson, "High Capacity Piles", *Proceedings*, *Lecture Series*, *Innovation in Foundation Construction*, *ASCE*, pp. 52, Illinois Section (1972).
[24] J. Konkol, "Numerical estimation of the pile toe and shaft unit resistances during the installation process in sands", *Studia Geotechnica et Mechanica*, vol. 37 No. 1, pp. 38–44 (2015).
[25] J.L. Briaud, "Geotechnical Engineering: Unsaturated and saturated soils", pp. 575, *Wiley*, New Jersey (2013).
[26] Z. Meyer, K. Żarkiewicz, "Pile shaft resistance formation mechanism, experimental analysis", *Regionalne Problemy Inżynierii Środowiska*, Szczecin, 2017, [in Polish].
[27] K. Żarkiewicz, PhD: "Analysis of pile shaft bearing capacity formation in non-cohesive soils based on laboratory model investigation", *West Pomeranian University Of Technology in Szczecin*, Szczecin 2017, [in Polish].
[28] G. Szmechel, PhD: "Boundary pile bearing capacity estimation based on static pile load test in limited range", *West Pomeranian University Of Technology in Szczecin*, Szczecin 2014, [in Polish].